Soldering & Surface Mount Technology

Compressive sensing for noisy solder joint imagery based on convex optimization

Huihuang Zhao Jianzhen Chen Shibiao Xu Ying Wang Zhijun Qiao

Compressive sensing for noisy solder joint imagery based on convex optimization

Huihuang Zhao and Jianzhen Chen
Department of Computer Science, HengYang Normal University, HengYang, China
Shibiao Xu
National Laboratory of Pattern Recognition, Institute of Automation, Chinese Academy of Sciences, Beijing, China
Ying Wang
Department of Computer Science, HengYang Normal University, HengYang, China, and
Zhijun Qiao
Department of Mathematics, University of Texas-Pan American, Edinburg, TX, USA

Abstract

Purpose – The purpose of this paper is to develop a compressive sensing (CS) algorithm for noisy solder joint imagery compression and recovery. A fast gradient-based compressive sensing (FGbCS) approach is proposed based on the convex optimization. The proposed algorithm is able to improve performance in terms of peak signal noise ratio (PSNR) and computational cost.

Design/methodology/approach – Unlike traditional CS methods, the authors first transformed a noise solder joint image to a sparse signal by a discrete cosine transform (DCT), so that the reconstruction of noisy solder joint imagery is changed to a convex optimization problem. Then, a so-called gradient-based method is utilized for solving the problem. To improve the method efficiency, the authors assume the problem to be convex with the Lipschitz gradient through the replacement of an iteration parameter by the Lipschitz constant. Moreover, a FGbCS algorithm is proposed to recover the noisy solder joint imagery under different parameters.

Findings – Experiments reveal that the proposed algorithm can achieve better results on PNSR with fewer computational costs than classical algorithms like Orthogonal Matching Pursuit (OMP), Greedy Basis Pursuit (GBP), Subspace Pursuit (SP), Compressive Sampling Matching Pursuit (CoSaMP) and Iterative Re-weighted Least Squares (IRLS). Convergence of the proposed algorithm is with a faster rate O(k*k) instead of O(1/k).

Practical implications – This paper provides a novel methodology for the CS of noisy solder joint imagery, and the proposed algorithm can also be used in other imagery compression and recovery.

Originality/value – According to the CS theory, a sparse or compressible signal can be represented by a fewer number of bases than those required by the Nyquist theorem. The new development might provide some fundamental guidelines for noisy imagery compression and recovering.

Keywords Noisy solder joint imagery, Compressive sensing (CS), Convex optimization, Gradient-based method, Orthogonal matching pursuit, Greedy basis pursuit, Subspace pursuit and compressive sampling matching pursuit, Iterative re-weighted least squares

Paper type Research paper

1. Introduction

In recent years, the compressive sensing (CS) theory has played an important role in sampling paradigm and data and signal processing. A sparse or compressible signal can be represented by a fewer number of bases than those required by the Nyquist theorem when it is mapped to the space with bases incoherent to the sparse data space (Donoho, 2006; Donoho *et al.*, 2006). In the literature, most references talk about raw data compression and imagery reconstruction on the basis of the CS theory.

The CS has successfully been applied in quite a wide variety of areas, including photography (Huynh-Thu and Ghanbari, 2008), shortwave infrared cameras, optical system research (Donoho *et al.*, 2012), audio and music processing (Godsill *et al.*, 2007) and MRI Vasanawala *et al.*, 2010). Particularly, in Jørgensen *et al.* (2012), an iterative image reconstruction method in X-ray CT is proposed through CS. Bhattacharya *et al.* (2007) provided a method of fast encoding for Synthetic Aperture Radar (SAR) raw data by using the CS theory to complete SAR raw data sparsity and processing.

The current issue and full text archive of this journal is available on Emerald Insight at: **www.emeraldinsight.com/0954-0911.htm**

Soldering & Surface Mount Technology
28/2 (2016) 114–122
© Emerald Group Publishing Limited [ISSN 0954-0911]
[DOI 10.1108/SSMT-09-2014-0017]

This work was supported by National Natural Science Foundation of China (61503128), Scientific Research Fund of Hunan Provincial Education Department (14B025,13C074), Science and Technology development project of HengYang (2015KJ28), Key Construction Disciplines of the Hunan Province during the Twelfth Five-Year Plan Period, Open fund project of Hunan Provincial Key Laboratory for Technology and Application of Cultural Heritage Digitalization (JL14K04) and Open Projects Program of National Laboratory of Pattern Recognition (201407330).

Received 28 September 2014
Revised 21 December 2014
29 April 2015
30 July 2015
Accepted 22 September 2015

Nowadays, surface mount technology (SMT) components have widely been used in the electronics industry. The surface-related defects include pseudo-solder (Wu and Zhang, 2011), insufficient solder, component shift, wrong component and tombstoning (Janoczki *et al.*, 2010). To detect them, some approaches such as automatic optical inspection (AOI) and X-ray inspection, etc., have been applied to SMT-based production. The methods have proved to be a useful supplement to circuit and functional testing (Xie *et al.*, 2011, Benedek *et al.*, 2013). However, SMT brings a great challenge for defect inspection with the development of solder bumps towards ultra-fine pitch and high density. The traditional non-destructive detection methods are insufficient for solder joint assessment. This is not only due to their own factors, including slow speed and low precision, but also due to external interference, including light and noise (Ong *et al.*, 2008). The solder joint image could be corrupted with noise during the image capturing process (Said *et al.*, 2011). The noise could greatly affect the inspection result (Sankaran *et al.*, 1998). The common noises possibly existing in solder joint images include Gaussian noise, Thermal noise, Salt and Pepper noise, Rand noise and so on.

To improve the inspection rate of defects, some image processing technologies, such as image compression, image enhancing and image filtering, are used in AOI and Solder Paste Inspection (SPIs) (Xiong *et al.*, 2012). The authors (Lu *et al.*, 2011) propose an improved median filter to remove the Gaussian noise in solder joint defect inspection. In the work by Said *et al.* (2011), median filter is used in eliminating salt and pepper noise in solder joint images. Usually, wavelet transform and wavelet package transform are cast into image compression (Karami *et al.*, 2012; Bayazit, 2011). Due to the requirement for steadily increasing resolution for the imagery acquisition platforms, the amount of image data produced is managed by storage capabilities and the slow inspection speed (Wu *et al.*, 2013). In our previous work (Zhao *et al.*, 2014), an improved block CS algorithm was developed for solder joint imagery compression and recovery, and it achieved a better performance.

In the literature, there are few works talking about noisy solder joint imagery data compression and reconstruction based on the CS theory. In this paper, we present a fast-speed, high-precision CS algorithm for noisy solder joint imagery compression and recovery. In our approach, we study data compression and reconstruction through using the convex optimization and a fast gradient-based compressive sensing (FGbCS).

The whole paper is organized as follows. The signal recovery based on convex optimization problems is described in Section 2. In Section 3, the noisy solder joint imagery reconstruction is investigated through the adoption of the CS with gradient-based method, and a fast FGbCS recovery algorithm is discussed in detail. In Section 4, some experimental results are shown and compared for different methods. Conclusions and open problems are summarized in Section 5.

2. Convex optimization with gradient-based method

The convex optimization problem we want to deal with is one of the following (Boyd and Vandenberghe, 2009):

$$\begin{array}{ll} \text{minize} & g_0(x) \\ \textit{subject to} & g_i(x) \le b_i, i = 1, 2, \ldots, m, \end{array} \tag{1}$$

where the functions $g_0, \ldots, g_m$: $R^n \to R$ are convex, that is, satisfy:

$$g_i(\alpha x + \beta y) \le \alpha g_i(x) + \beta g_i(y) \tag{2}$$

for all $x, y \in R$ and all $\alpha, \beta \in R$ with $\alpha+\beta=1, \alpha\geq0, \beta\geq0$.

One of the simplest methods to solve equation (1) is the gradient algorithm to generate a sequence x_k via:

$$x_0 \in R^n, x_k = x_{k-1} - t_k \nabla g(x_{k-1}), \tag{3}$$

where $t_k > 0$ is a suitable step size. It is very well known that the gradient iteration equation (3) can be regarded as a proximal regularization (Figueiredo *et al.*, 2007) of the linearized function g at x_{k-1} and equivalently rewritten as:

$$x_k = \arg\min_x \left\{ g(x_{k-1}) + <(x - x_{k-1}), \nabla g(x_{k-1}) > + \frac{1}{2t_k}\|x - x_{k-1}\|_2^2 \right\}. \tag{4}$$

Applying the same idea to the non-smooth l_1 regularized problem:

$$\min\{g(x) + \lambda\|x\|_1 : x \in R^n\} \tag{5}$$

leads to the following iterative scheme:

$$x_k = \arg\min_x \left\{ g(x_{k-1}) + <x - x_{k-1}, \nabla g(x_{k-1}) > + \frac{1}{2t_k}\|x - x_{k-1}\|_2^2 + \lambda\|x\|_1 \right\}. \tag{6}$$

After constant terms are ignored, equation (6) can be rewritten as:

$$x_k = \arg\min_x \left\{ \frac{1}{2t_k}\|x - (x_{k-1} - t_k \nabla g(x_{k-1}))\|_2^2 + \lambda\|x\|_1 \right\} \tag{7}$$

Many researchers have investigated equation (7) through various techniques. A more general result can be found in the study by Beck and Teboulle (2009) with its convergence O(1/K).

In the following, we convert the problem of CS for noisy solder joint imagery to a convex minimization model and take advantage of a gradient-based method to improve convergence and efficiency.

3. Compressive sensing for noisy solder joint imagery

The CS theory has three major steps to reconstruct an image: construction of k-sparse representation, compression and reconstruction. In the first step, k is the number of the non-zero entries of sparse signals. Most natural signals can be made sparse by applying orthogonal transforms, such as Wavelet Transform, Fast Fourier Transform and discrete cosine transform (DCT) (Candes and Wakin, 2008). In the second step, compression, the random measurement matrix is utilized to the sparse signal according to certain equations. The third step is the sparse signal reconstruction. The details of CS theory can be seen in the study by Zhao *et al.* (2014).

3.1 Noisy solder joint imagery optimization with Lipschitz gradient

Given a noise solder joint imagery, the noise is added into the compressive measurement vector as follows:

$$y = \Phi s + noise, \tag{8}$$

where *noise* is an M-dimensional noise vector.

Let us think about an objective function $F(x) = g(x) + n(x)$, where $g(x)$ is a composite type convex function, and its Lipschitz gradient is shown as follows (Nesterov, 1983):

$$\|g(x) - \nabla g(y)\|_2 \nabla\| \leq L(g)\, \|x - y\|_2 \text{ for every } x,\ y \tag{9}$$

where $\|.\|$ denotes the standard Euclidean norm and $L(g) > 0$ is the Lipschitz constant of ∇g. Let us approximate the function $F(x)$ at point x_{k-1} by the following quadratic function:

$$Q_L(x, x_{k-1}) = g(y) + <x - x_{k-1}, \nabla g(x_{k-1})> + \frac{L}{2}\|x - x_{k-1}\|_2^2 + n(x), \tag{10}$$

which admits a unique minimizer:

$$PL(x_{k-1}) = \arg\min_x \{Q_L(x, x_{k-1}), x \in R^n\} \tag{11}$$

Simple algebra shows that (ignoring constant terms inx_{k-1}):

$$PL(x_{k-1}) = \arg\min_x \left\{\frac{L}{2}\|x - (x_{k-1} - \frac{1}{L}\nabla g(x_{k-1}))\|_2^2 + n(x)\right\}. \tag{12}$$

Clearly, in equation (4), x_k can be replaced by:

$$x_k = PL(x_{k-1}) \tag{13}$$

where L is $1/t_k$. Apparently, as long as the constant L in equation (8) is taken no less than Lipschitz constant $L(g)$, it follows that:

$$g(x) + n(x) \leq g(x_{k-1}) + < \nabla g(x_{k-1}), x - x_{k-1}> + \frac{L}{2}\|x - x_{k-1}\|_2^2 + n(x). \tag{14}$$

In the above calculation, $1/t_k$ is replaced by a constant L which is related to the Lipschitz constant $L(g)$. One may verify that the right-hand side of equation (14) is exactly equal to $Q_L(x, y)$ in equation (10). In other words, $Q_L(x, y)$ is an easier-to-deal-with convex upper bound of the objective function $F(\boldsymbol{x})$. By minimizing the upper bound, $Q_L(x, y)$ together with x_k given by equation (13) offers a tight upper bound of $F(\boldsymbol{x})$, provided $L \geq L(f)$.

3.2 Fast gradient-based compressive sensing algorithm for noisy solder joint imagery

The major challenge in the algorithm of compressive sampling is to approximate a noise signal for given samples in a vector form. In our method, equation (8) is often used more naturally to study the following problem:

$$\min\ mize\ \|\Phi\Psi^T x - y\|_2^2 + \lambda\|x\|_1 \tag{15}$$

where Ψ is an $N \times N$ orthogonal basis matrix and Φ is an $M \times N$ random measurement matrix ($M < N$).

Let us begin with equation (15). Assumed equation (15) is convex with smooth Lipschitz gradient. For any $L > 0$, the CS of noisy solder joint imagery formulated by equation (15) becomes:

$$x_k = \arg\min_x \left\{\frac{L}{2}\|x - x_{k-1}\|^2 + \lambda\|x\|_1\right\}, \tag{16}$$

where $x_k = PL(x_{k-1})$. So:

$$x_k = \arg\min_x \left\{\frac{L}{2}\|x - (x_{k-1} - \frac{1}{L}\nabla f(x_{k-1}))\|_2^2 + \lambda\|x\|_1\right\} \tag{17}$$

or equivalently:

$$x_k = \arg\min_x \left\{\frac{L}{2}\|x - d_k\|_2^2 + \lambda\|x\|_1\right\}, \tag{18}$$

where $d_k = x_{k-1} - 1 / L\nabla f(x_{k-1})$. By equation (15), d_k can be rewritten as:

$$d_k = x_{k-1} - \frac{1}{L}(\Phi\Psi^T)^T(\Phi\Psi^T x_{k-1} - y) \tag{19}$$

Because both the one-norm and the two-norm are separable, that is, each of them is only the sum of n *non-negative* terms that only involves a *single* (scalar) variable, iterated x_k in equation(17) can be computed by a straightforward shrinkage step (assuming d_k in equation(19) has been figured out) through:

$$x_k = \Gamma_{\lambda L}(d_k) \tag{20}$$

where Γ_α is a shrinkage operator which maps R^n to R^n with the i -th entry of the output vector given by:

$$\Gamma_\alpha(d)\big|_i = (|d_i| - \alpha)_+ \operatorname{sgn}(d_i) \tag{21}$$

where $(u)_+ = \max(u, 0)$.

As per the fact described above, we may call the approach a FGbCS for noisy solder joint imagery reconstruction. The detailed procedure in the algorithm is shown as follows in Algorithm 1:

Algorithm 1 FGbCS (Φ,Ψ, s, λ, K, M)

Input:

1 $L = L(g) - a Lipschitz\ constant\ of\ \nabla g(x)$ in equation(9);
2 A signal $s,\Psi \in R^{N\times N}$ is a signal sparse transform matrix, $s_p = \Psi s$;
3 A measurement matrix $\Phi \in R^{N\times N}$, $x = \Phi s_p$;
4 The iteration counter K and noise parameter λ, and M is the chosen row number of Φ.

Procedure
Initialize, $y_1 = x_0 \in R^n$, $t_1 = 1$.
If $1 \leq k \leq K$, compute

1 $x_k = PL(y_k)$ by solving the problem in equation (13).

2 $t_{k+1} = \dfrac{1+\sqrt{1+4t_k^2}}{2}$

3 $y_{k+1} = x_k + \left(\dfrac{t_k - 1}{t_{k+1}}\right)(x_k - x_{k-1})$

End
Output:
A sparse approximation x_k of the target signal and then reconstruction of the resulting signal $s' = \Psi^T x_k$.

Compared with other reconstruction algorithms, the proposed algorithm has the following characteristics:

- The CS for a noise signal may be estimated as a convex minimization problem, and the gradient-based method is used to solve the problem.
- The problem of noise signal reconstruction is assumed to be the convex with the Lipschitz gradient. An iteration parameter $1/t_k$ is replaced by a constant 1/L, which is related to the Lipschitz constant L(f).
- According to the fact described in Nesterov (1983), one can easily verify that the convergence of FGbCS is $O(1/k^2)$.

4. Experimental and results

To evaluate the quality of the reconstructed results, the mean square error (MSE) and peak signal to noise ratio (PSNR) are used for the comparison in this paper. They are defined by (Huynh-Thu and Ghanbari, 2008):

$$MSE = \frac{1}{M \times N} \sum_{i=1}^{M} \sum_{j=1}^{N} (\hat{f}(i,j) - f(i,j))^2 \tag{22}$$

$$\mathrm{PSNR} = 10\log_{10}\left(\frac{255^2}{MSE}\right) \tag{23}$$

Figure 1 Original image and sparse image

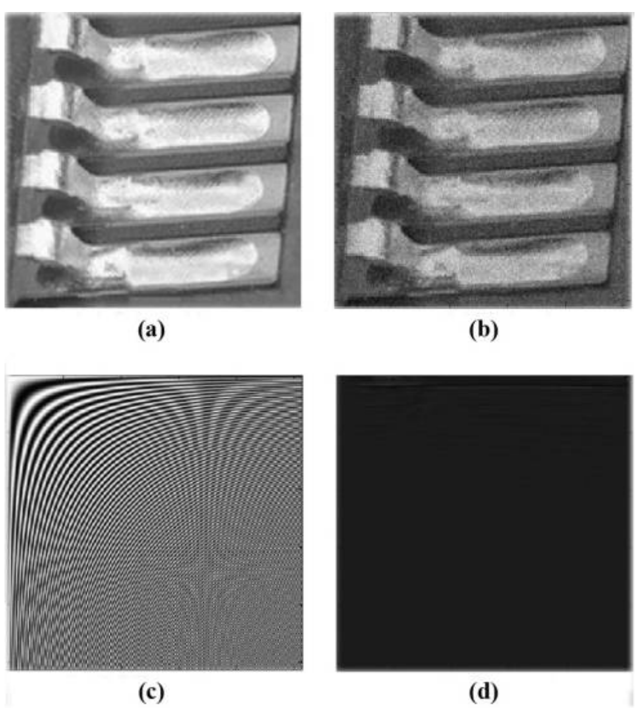

Notes: (a) Original image; (b) noise image; (c) DCT matrix; (d) sparse image

Figure 2 Reconstruction result by using the different methods

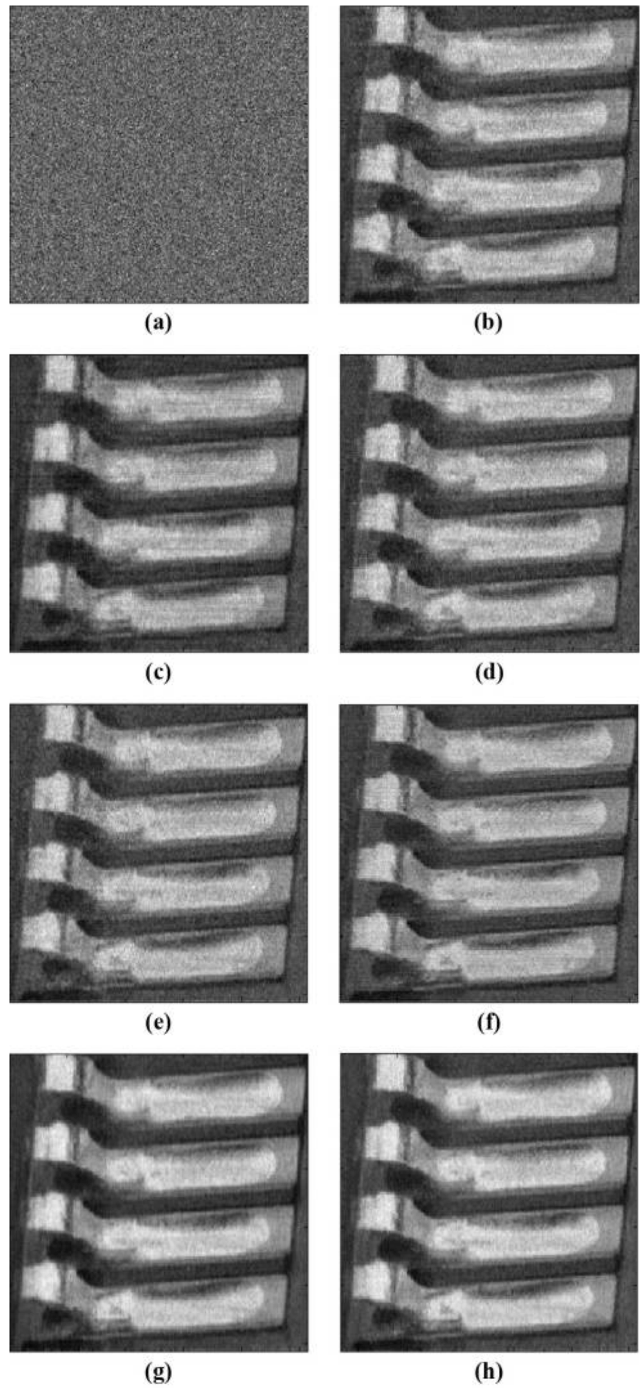

Notes: (a) Random measurement matrix; (b) OMP; (c) GBP; (d) SP; (e) CoSaMP; (f) IRLS; (g) FGbCS (K = 40); (h) FGbCS (K = 80) where M and N are the image dimensional numbers, $\hat{f}$ is the de-noised image and f is the original noiseless image. In our study, the PSNR is used to compare with the experiment results which were implemented on a Pentium IV with 3.2 GHz CPU and 2,048 MB RAM.

During the running of these experiments, several classical algorithms, such as Orthogonal Matching Pursuit (OMP) (Cai and Wang, 2011), Greedy Basis Pursuit (GBP) (Huggins and Sucker, 2007), Subspace Pursuit (SP) (Dai and Milenkovic, 2009), Compressive Sampling Matching Pursuit (CoSaMP) (Davenport *et al.*, 2013) and Iterative Re-weighted Least Squares (IRLS) (Daubechies *et al.*, 2010), were selected to compare with the FGbCS.

Table I. Reconstruction result in peak signal noise ratio and runtime by using different methods

Methods/performance	PSNR (dB)	Runtime (s)
OMP	24.3983	3.583
GBP	24.9407	32.445
SP	25.1229	20.107
CoSaMP	25.1848	36.158
IRLS	27.0805	96.150
FGbCS (λ = 20 K = 40)	27.6147	4.5080
FGbCS (λ = 20 K = 80)	28.2991	5.1140

An original gull-wing leaded solder joint image was used as a test image in Figure 1(a) (size 256 × 256). Rand noise is one common noise in images, and the original image is degraded by Rand noise ($\sigma = 10$) in Figure1(b). The sparse transform DCT matrix and sparse image are shown in Figure 1(c and d).

When the row of measurement matrix is M = 230, the reconstruction results based on different algorithms are shown in Figure 2(a-e). The reconstruction result based on FGbCS with $\lambda = 20$ and K = 40 is shown in Figure 2(g) when $\lambda = 20$ and K = 80.

One can see by the comparison of Figure 1(b-g) that our method can yield better results in PSNR than other CS algorithms. The reconstruction result in PSNR and runtime for our method and other methods are shown in Table I.

Figure 3 Performance comparisons in rand noises solder joint imagery reconstruction

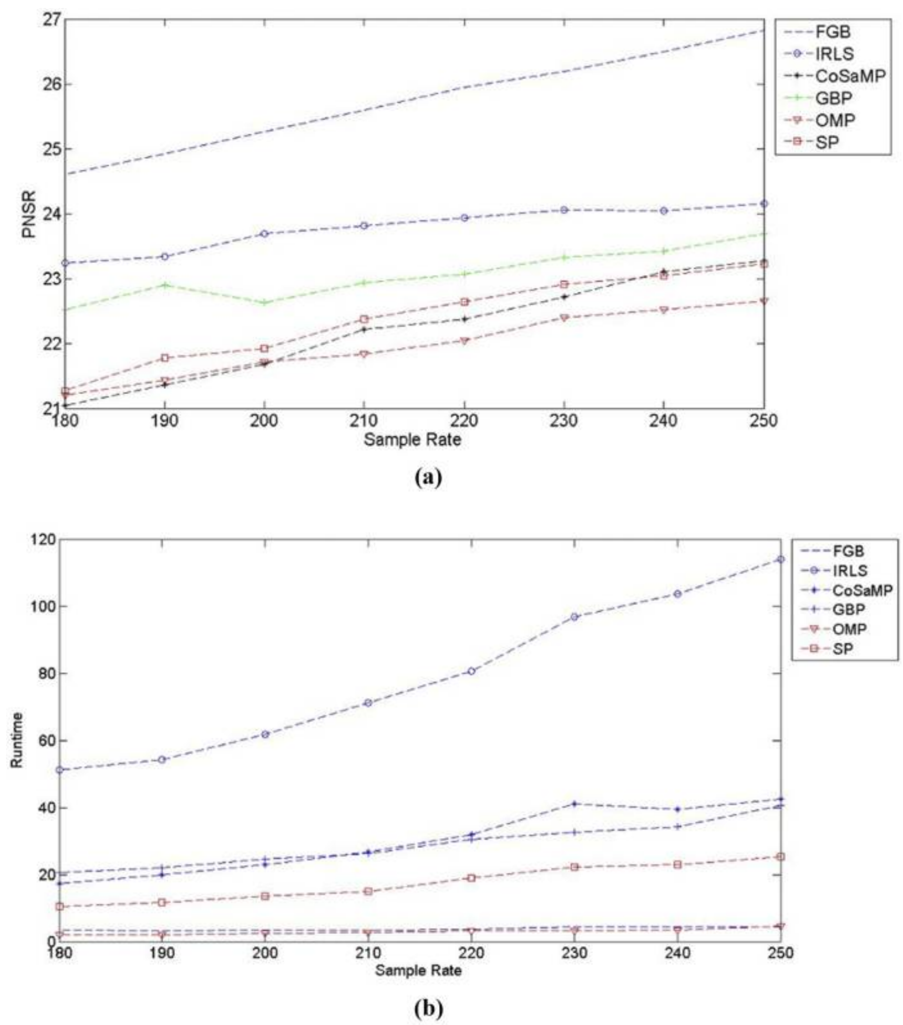

Notes: (a) PSNR comparison; (b) runtime comparison

From Table I, we know that the FGbCS algorithm spends the least runtime than other methods. IRLS, SP, CoSaMP and GBP spend more time in noisy solder joint imagery reconstruction.

To compare their reconstruction performances in detail, more experiments were also performed. When Rand noise $\sigma = 15$, the reconstruction runtime and PSNR with different rows of measurement matrices are shown in Figure 3(a and b). While implementing the FGbCS, we set $\lambda = 20$ and K = 40.

Then, more experiments were done by adding salt-and-pepper noise (the noise density was 0.01), as shown in Figure 1(a). During the experiments, we set the row of measurement matrix M = 230, the reconstruction runtime and PSNR with different Gaussian are shown in Figure 4(a and b). While implementing the FGbCS, we set $\lambda = 20$ and K = 80.

From Figures 3 and 4, one can see that:

- among those methods, the FGbCS can obtain better reconstruction result in terms of PSNR as compared to OMP, SP, CoSaMP, GBP and IRLS;
- the proposed method can run as fast as OMP methods in noisy imagery reconstruction and is faster than SP, CoSaMP, GBP and IRLS methods;
- with the increasing measurement matrix rows, the proposed method can generate better reconstruction accuracy with only a few runtime changes; and
- the proposed method has an improved performance and good resilience to Rand noise and salt-and-pepper noise.

To compare the relationship between parameter λ and K in FGbCS, more experiments needed to be carried out. When the solder joint is degraded by Rand noise $\sigma = 10$, we set K = 60 and the row of measurement matrix M = 230. The reconstruction of PSNR with different λ is shown in Figure 5(a). If we set $\lambda = 10$, then the row of measurement matrix M = 230 and the reconstruction of PSNR with different K is shown in Figure 4(b).

One may see from Figure 5 that if K = 60 and M = 230, then FGbCS is able to yield a better performance when λ is around 15. If $\lambda = 10$ and M = 230, then FGbCS can give a better result when K > 50.

Figure 4 Performance comparisons in salt-and-pepper noise solder joint imagery reconstruction

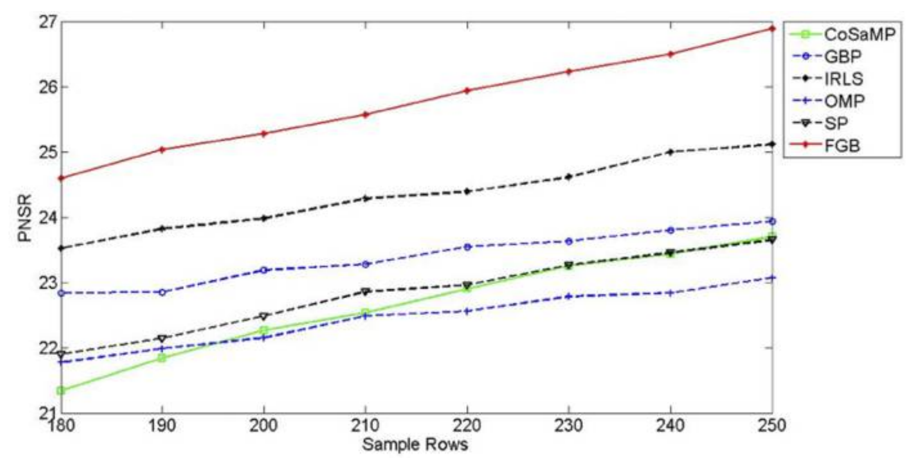

(a)

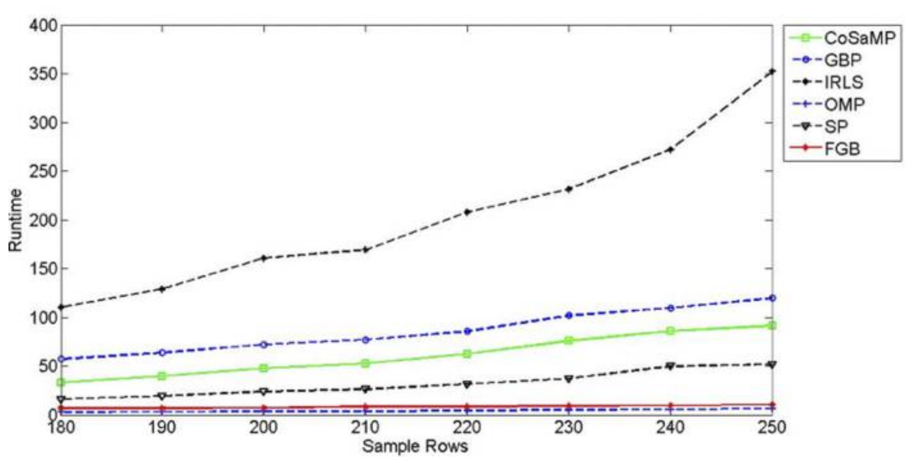

(b)

Notes: (a) PSNR comparison; (b) runtime comparison

Figure 5 PSNR comparisons with different parameters

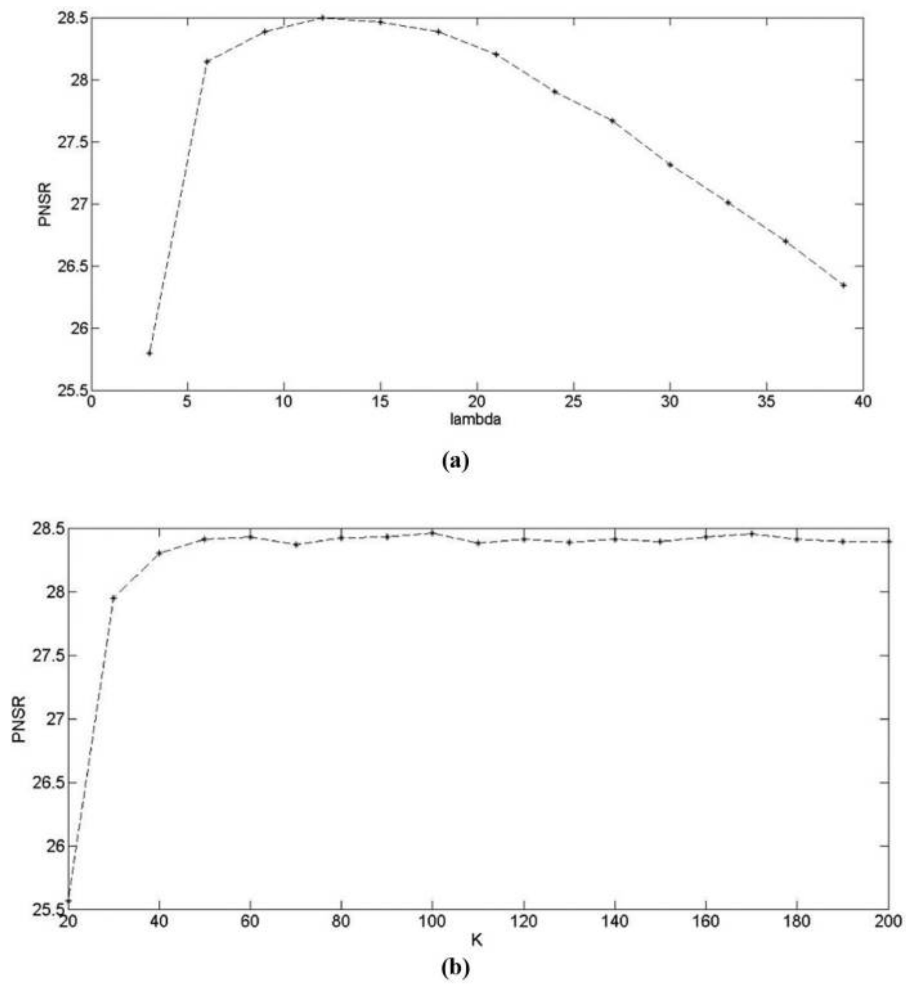

Notes: (a) K = 60, M = 230; (b) λ = 10, M = 230

5. Conclusion

There is a challenging research problem in compressive sampling to approximate a noise signal given a vector of samples. This paper focuses on the development of compression and reconstruction methods for noisy solder joint imagery based on convex optimization. FGbCS is proposed in our paper. On the one hand, we deal with the noisy imagery reconstruction as a convex minimization problem and provide a new method. On the other hand, to improve the efficiency, we consider the problem of noise signal reconstruction assumed to be convex with Lipschitz gradient. The step size in gradient iteration is replaced by a constant 1/L, which is related to the Lipschitz constant. The convergence of proposed algorithm is reduced from O(1/k) to $O(1/k^2)$. In our future studies, more relationships between parameter λ and K will be needed to be tracked. The FGbCS has an improved performance and good resilience to rand noise and salt-and-pepper noise.

References

Bayazit, U. (2011), "Adaptive spectral transform for wavelet-based color image compression", *IEEE Transactions on Circuits and Systems for Video Technology*, Vol. 21 No. 7, pp. 983-992.

Beck, A. and Teboulle, M. (2009), "A fast iterative shrinkage-thresholding algorithm for linear inverse problems", *SIAM Journal on Imaging Sciences*, Vol. 2 No. 1, pp. 183-202.

Benedek, C.S., Krammer, O., Janóczki, M. and Jakab, L. (2013), "Solder paste scooping detection by multi-level visual inspection of printed circuit boards", *IEEE Transactions on Industrial Electronics*, Vol. 60 No. 6, pp. 2318-2331.

Bhattacharya, S., Blumensath, T., Mulgrew, B. and Davies, M. (2007), "Fast encoding of synthetic aperture radar raw data using compressed sensing", *2007 IEEE/SP 14th Workshop on Statistical Signal Processing, Madison, WI, 26-29 August*, pp. 448-452.

Boyd, S. and Vandenberghe, L. (2009), *Convex Optimization*, Cambridge University Press, Cambridge.

Cai, T.T. and Wang, L. (2011), "Orthogonal matching pursuit for sparse signal recovery with noise", *IEEE Transaction on Information Theory*, Vol. 57 No. 7, pp. 4680-4688.

Candes, E.J. and Wakin, M.B. (2008), "An introduction to compressive sampling", *IEEE Signal Processing Magazine*, Vol. 25 No. 2, pp. 21-30.

Dai, W. and Milenkovic, O. (2009), "Subspace pursuit for compressive sensing signal reconstruction", *IEEE Transactions on Information Theory*, Vol. 55 No. 5, pp. 2230-2249.

Daubechies, I., DeVore, R., Fornasier, M. and Güntürk, C.S. (2010), "Iteratively reweighted least squares minimization for sparse recovery", *Communications on Pure and Applied Mathematics*, Vol. 63 No. 1, pp. 1-38.

Davenport, M.A., Needell, D. and Wakin, M.B. (2013), "Signal space CoSaMP for sparse recovery with redundant dictionaries", *IEEE Transactions on Information Theory*, Vol. 9 No. 9, pp. 1-18.

Donoho, D.L. (2006), "Compressed sensing", *IEEE Transactions on Information Theory*, Vol. 52 No. 4, pp. 1289-1306.

Donoho, D.L., Elad, M. and Temlyakov, V.N. (2006), "Stable recovery of sparse overcomplete representations in the presence of noise", *IEEE Transactions on Information Theory*, Vol. 52 No. 1, pp. 6-18.

Donoho, D.L., Tsaig, Y., Drori, I. and Starck, J.L. (2012), "Sparse solution of underdetermined systems of linear equations by stagewise orthogonal matching pursuit", *IEEE Transactions on Information Theory*, Vol. 58 No. 2, pp. 1094-1121.

Figueiredo, M.A., Nowak, R.D. and Wright, S.J. (2007), "Gradient projection for sparse reconstruction: application to compressed sensing and other inverse problems", *IEEE Journal of Selected Topics in Signal Processing*, Vol. 1 No. 4, pp. 586-597.

Godsill, S.J., Cemgil, A.T., Févotte, C. and Wolfe, P.J. (2007), "Bayesian computational methods for sparse audio and music processing", *Signal Processing Conference, 2007 15th European*. IEEE, pp. 345-349.

Huggins, P.S. and Sucker, S.W. (2007), "Greedy basis pursuit", *IEEE Transactions on Signal Processing*, Vol. 55 No. 7, pp. 3760-3772.

Huynh-Thu, Q. and Ghanbari, M. (2008), "Scope of validity of PSNR in image/video quality assessment", *Electronics Letters*, Vol. 44 No. 13, pp. 800-801.

Janoczki, M., Borbiro, A., Nagy, S. and Jakab, L. (2010), "Illumination optimization for Quasi-Tombstone detection", *Micro and Nanosystems*, Vol. 2 No. 3, pp. 149-162.

Johnson, K.M., Block, W.F., Reeder, S.B. and Samsonov, A. (2012), "Improved least squares MR image reconstruction using estimates of k-Space data consistency", *Magnetic Resonance in Medicine*, Vol. 67 No. 6, pp. 1600-1608.

Jørgensen, J.H., Sidky, E.Y. and Pan, X. (2012), "Quantifying admissible undersampling for sparsity-exploiting iterative image reconstruction in X-ray CT", *IEEE Transactions on Medical Imaging*, Vol. 32 No. 2, pp. 460-473.

Karami, A., Yazdi, M. and Mercier, G. (2012), "Compression of hyperspectral images using discerete wavelet transform and tucker decomposition", *IEEE Journal of Selected Topics in Applied Earth Observations and Remote Sensing*, Vol. 5 No. 2, pp. 444-450.

Lu, X., Liao, G., Zha, Z., Xia, Q. and Shi, T. (2011), "A novel approach for flip chip solder joint inspection based on pulsed phase thermography", *NDT & E International*, Vol. 44 No. 6, pp. 484-489.

Nesterov, Y. (1983), "A method of solving a convex programming problem with convergence rate O (1/k2)", *Soviet Mathematics Doklady*, Vol. 27 No. 2, pp. 372-376.

Ong, T.Y., Samad, Z. and Ratnam, M.M. (2008), "Solder joint inspection with multi-angle imaging and an artificial neural network", *The International Journal of Advanced Manufacturing Technology*, Vol. 38 Nos 5/6, pp. 455-462.

Said, A.F., Bennett, B.L., Karam, L.J. and Pettinato, J.S. (2011), "Automated detection and classification of non-wet solder joints", *IEEE Transactions on Automation Science and Engineering*, Vol. 8 No. 1, pp. 67-80.

Sankaran, V., Kalukin, A.R. and Kraft, R.P. (1998), "Improvements to X-ray laminography for automated inspection of solder joints", *IEEE Transactions on, Components, Packaging, and Manufacturing Technology, Part C*, Vol. 21 No. 2, pp. 148-154.

Vasanawala, S.S., Alley, M.T., Hargreaves, B.A., Barth, R.A., Pauly, J.M. and Lustig, M. (2010), "Improved pediatric MR imaging with compressed sensing", *Radiology*, Vol. 256 No. 2, pp. 607-616.

Wu, F.P. and Zhang, X.M. (2011), "Inspection of pseudo solders for lead-free solder joints in PCBs", *Optics and Precision Engineering*, Vol. 19 No. 3, pp. 697-702.

Wu, H., Zhang, X., Xie, H., Kuang, Y. and Ouyang, G. (2013), "Classification of solder joint using feature selection based on bayes and support vector machine", *IEEE Transactions on components Packaging and Manufacturing Technology*, Vol. 3 No. 3, pp. 516-522.

Xie, H., Zhang, X., Kuang, Y. and Ouyang, G. (2011), "Solder joint inspection method for chip component using improved adaboost and decision tree", *IEEE Transaction on Components, Packaging and Manufacturing Technology*, Vol. 1 No. 12, pp. 218-227.

Xiong, G., Lu, J. and Wu, S. (2012), "New automatic optical inspection system for PCB", *Proceedings of the 2012 International Conference on Electronics, Communications and Control*, pp. 1270-1273.

Zhao, H., Wang, Y. and Qiao, Z. (2014), "Solder joint imagery compressive and recovery based on compressive sensing", *Soldering & Surface Mount Technology*, Vol. 26 No. 3, p. 4.

About the authors

Huihuang Zhao received his PhD degree from the School of Mechano-Electronic Engineering, Xidian University, China, in 2010. He is currently an Associate Professor in the Computer Science Department, Hengyang Normal University. His research interests include computer vision and surface mount technology. Huihuang Zhao is the corresponding author and can be contacted at: happyday.huihuang@gmail.com

Jianzhen Chen received his PhD degree in 2010. He is the Vice Dean of Computer Science Department and currently a Professor in the Computer Science Department, Hengyang

Normal University. His research interests include intelligent control and pattern recognition, GPU computing.

Shibiao Xu received the BS degree in information engineering from the Beijing University of Posts and Telecommunications, Beijing, China, in 2009 and the PhD degree in computer science from the Institute of Automation, Chinese Academy of Sciences, Beijing, China, in 2014. He is currently a Postdoctoral Researcher with the State Key Laboratory of Virtual Reality Technology and Systems, Beihang University, Beijing. His current research interests include computer vision and image-based three-dimensional scene reconstruction and understanding.

Ying Wang received her Master's degree from the School of Computer Science, Hunan University, China, in 2012. She is currently an Associate Professor in the Computer Science Department, Hengyang Normal University. Her research interests include image processing.

Zhijun Qiao received his PhD degree from Fudan University in 1997. He is a Professor of mathematics in the department of Mathematics, University of Texas-Pan American. His research interests include integrable systems, solitons, image PDEs and analysis, mathematical model, compressive sensing and radar image reconstructions.